Nuclear pore abnormalities in C9ORF72 ALS iPSC neurons and tissue alter nucleocytoplasmic protein trafficking

J. D. ROTHSTEIN[1,2,7], C.J. DONNELLY[1,3,4], K. ZHANG[2], A. HAEUSLER[6], J. C. GRIMA[7], E. DALEY[1], S.J. MILLER[1], L. W. OSTROW[2], J. WANG[6], R. SATTLER[1], T. LLOYD[2];
[1]Brain Science Institute, [2]Neurology, Johns Hopkins University, Baltimore, MD; [3]Department of Neurobiology, [4]Brain Institute, University of Pittsburgh, Pittsburgh, PA; [6]Department of Molecular Biology, Johns Hopkins University School of Public Health, Baltimore, MD; [7]Department of Neuroscience, Johns Hopkins University School of Medicine, Baltimore, MD

Introduction

A 'GGGGCC' repeat expansion in the C9ORF72 gene is the most common known genetic cause of familial and sporadic amyotrophic lateral sclerosis (ALS) and frontotemporal dementia (FTD). Similar to other repeat expansion disorders, the C9ORF72 GGGGCCexp RNA can sequester nuclear factors, including RNA binding proteins, and we hypothesize that these aberrant interactions are a major contributor of C9ORF72 neurotoxicity. Work from our laboratory has indicated that the GGGGCC RNA interacts with RanGAP1, a regulator of Ran-mediated nucleocytoplasmic protein trafficking. We now demonstrate that RanGap1 also biochemically binds to the GGGGCC repeat expansion with high affinity and specificity. We have also found that RanGAP1 is a robust suppressor of neurotoxicity in a Drosophila model system that overexpresses GGGGCC RNA. Consistent with a RanGAP1 loss-of-function model, the G4C2 Drosophila model shows reduced nuclear localization of NLS-containing reporters including TDP-43. iPS-neurons from C9ORF72 ALS patients exhibit perturbed nuclear/cytoplasmic Ran protein gradient and reduced nucleocytoplasmic import rates a reporter containing a classical NLS. Importantly, these nuclear transport deficits and protein mislocalization can be rescued by treating the C9ORF72-patient derived iPS-neurons with antisense oligonucleotides that target GGGGCC repeat-containing RNAs. ASOs or small molecules that bind G-quartet RNA structures to prevent any interaction with endogenous proteins also rescue neurotoxicity in the Drosophila model. Supportive of a dysfunctional nuclear pore complex that underlies C9ORF72 ALS pathogenesis, we also observe pathologic aggregates of nuclear pore proteins including nup 205, nup 107 and RanGAP1 in the motor cortex and cerebellum of C9ORF72 ALS patients. Taken together, these studies strongly support a gain-of-function mechanism underlying C9ORF72 neurodegeneration. Moreover, we show that the toxic GGGGCCexp RNA acts at the nuclear pore to disrupt the nuclear import of classical NLS-containing proteins.

Methods

Fibroblast Collection, Reprogramming, and iPS Differentiation to Neurons: Patient fibroblasts were collected at Johns Hopkins Hospital with patient's consent (IRB protocol: NA_00021979) or by Dr. Pentti Tienari at the Helsinki University Central Hospital. **Collection of Human Autopsied Tissue**: Human autopsied tissue, collected with Institutional Review Board and ethics approval. **Antisense Oligonucleotide Treatment:** Modified 2'-methoxyethyl (MOE)/DNA ASOs were generated by Isis Pharmaceuticals. ***Drosophila* Assays:** All *Drosophila* work was performed by Ke Zhang, Ph.D. from the Lloyd Lab at JHU. **Microscopy and Image Analysis:** Z-stack images were taken on a Zeiss Axioimager with the Apotome tool or a Zeiss LSM700 laser scanning confocal microscope matched exposure times or laser settings and normalized within their respective experiment. **FRAP Analysis**: iPS neurons were transduced with a LV-NLS-tdTomato-NES at 45 DIV and imaging was performed at 51 – 60 DIV. Cells were images three times at 3 second intervals and then bleached at 50% laser power (Zeiss LSM 700) for 30 iterations. Images were taken every 3 seconds for 8 minutes. Analysis was performed by normalziing the pre- and post-bleach signals at 100 and 0%, respectively then accounting for global bleaching by normalizing each value to an unbleached area. **Statistical Analysis**: Statistical analysis was performed using the Student's t-test or One-Way Analysis of Variance with the Turkey's or Dunnet's posthoc test and the Prism 6 software (GraphPad Software, Inc).

Results

Figure 1. RanGAP1 is a modifier of G_4C_2 RNA-mediated toxicity and binds (G_4C_2) RNA

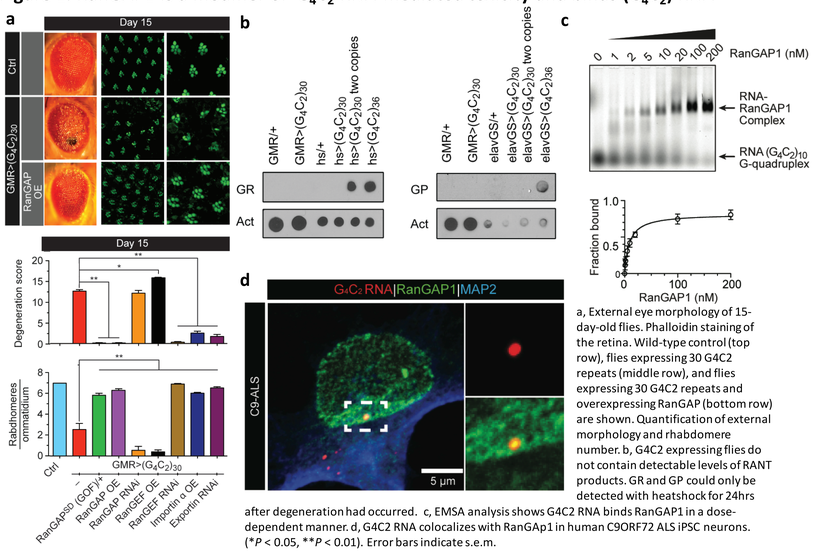

a, External eye morphology of 15-day-old flies. Phalloidin staining of the retina. Wild-type control (top row), flies expressing 30 G4C2 repeats (middle row), and flies expressing 30 G4C2 repeats and overexpressing RanGAP (bottom row) are shown. Quantification of external morphology and rhabdomere number. b, G4C2 expressing flies do not contain detectable levels of RANT products. GR and GP could only be detected with heatshock for 24hrs after degeneration had occurred. c, EMSA analysis shows G4C2 RNA binds RanGAP1 in a dose-dependent manner. d, G4C2 RNA colocalizes with RanGAp1 in human C9ORF72 ALS iPSC neurons. (*P < 0.05, **P < 0.01). Error bars indicate s.e.m.

Figure 2. RanGAP1 and nuclear pore proteins are mislocalized in C9ORF72 ALS motor cortex

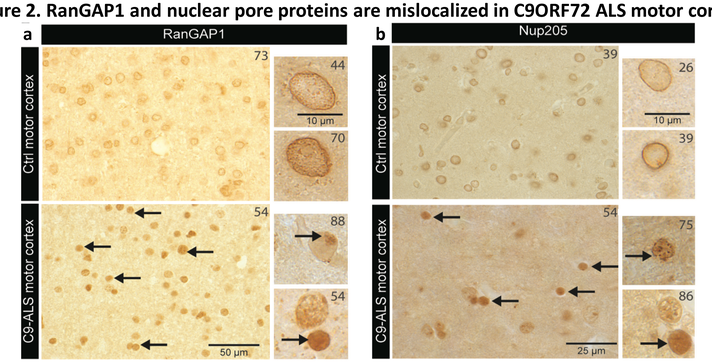

a, RanGAP1 immunostaining in non-neurological disease control and C9ORF72 ALS motor cortex showing intense nuclear localization (arrows) and aberrant nuclear aggregates. b, Abnormal nuclear localization of Nup205 in C9ORF72 human motor cortex cells.

Figure 3. Impaired nuclear/cytoplasmic RanGTPase gradient in C9ORF72 iPSC neurons

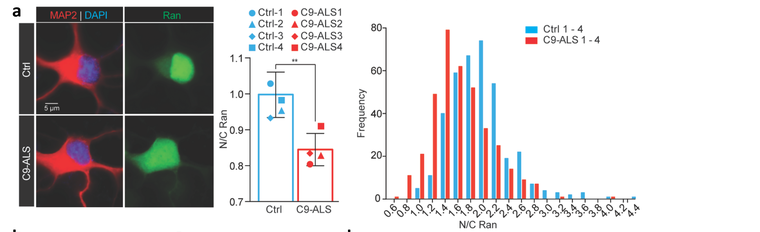

a, iPSC neurons from control and C9-ALS patients showing mislocalization of Ran to the cytoplasm in C9-ALS iPSC neurons. Quantification of N/C Ran gradient in neurons from four control and four C9-ALS iPS lines when normalized to control. N/C Ran ratio is reduced in C9-ALS neurons. Each symbol represents mean of up to 228 neurons per line. Bar indicates mean N/C Ran of four control or C9-ALS lines; N/C Ran histogram shows higher frequency of lower N/C ratios in four C9-ALS lines as compared to the four control lines. N/C ratios are presented as raw values. b, C9-ALS ChAT$^+$ neurons show similar reduction of N/C Ran. N/C Ran is normalized to controls and up to 60 neurons were tested per line. c, Overexpression of RanGAP1–GFP rescues the N/C Ran ratio in C9-ALS iPSC neurons. d, ER stress does not induce Ran mislocalization in control iPSC neurons despite elevated activated Caspase 3 in the soma.(**P < 0.01, ****P < 0.0001). Error bars indicate s.e.m.

Figure 4. Nucleocytoplasmic trafficking is disrupted in C9ORF72 ALS iPSC neurons

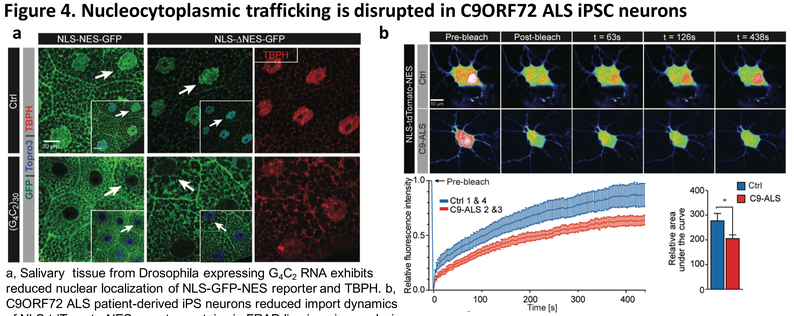

a, Salivary tissue from Drosophila expressing G_4C_2 RNA exhibits reduced nuclear localization of NLS-GFP-NES reporter and TBPH. b, C9ORF72 ALS patient-derived iPS neurons reduced import dynamics of NLS-tdTomato-NES reporter protein via FRAP live imaging analysis.

Figure 5: C9ORF72 ALS iPSC neurons show enhanced cytoplasmic TDP-43

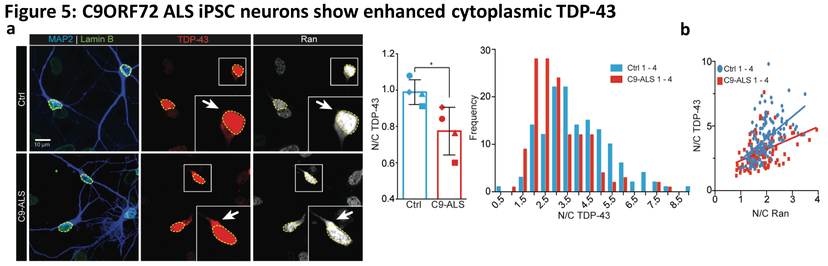

a, Representative images of control and C9-ALS iPSC neurons. Arrows indicate higher cytoplasmic Ran and TDP-43 signals. **e**, Quantification of mean N/C ratio of TDP-43 of four control and four C9-ALS lines when normalized to controls. Each symbol represents up to 49 neurons per line. Error bars indicate s.d. **f**, Histogram shows higher frequency of lower N/C TDP-43 ratio. N/C ratios are presented as raw values. **g**, N/C TDP-43 directly correlates with N/C Ran ratio across all lines tested. N/C TDP-43 versus N/C Ran: control, P < 0.0001, r^2 = 0.2980; C9-ALS, P < 0.0001, r^2 = 0.1657. *P < 0.05; **P < 0.01; ***P < 0.001.

Figure 6. Therapeutic rescue of nucleocytoplasmic import deficits and (G_4C_2)-mediated degeneration

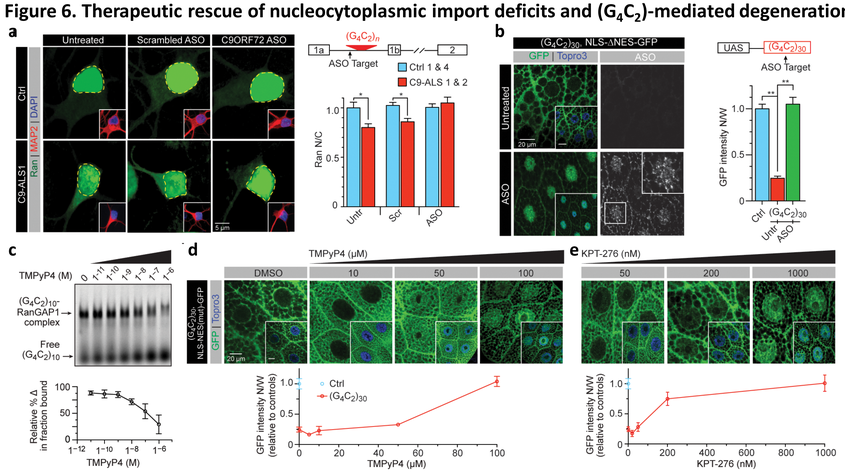

a, Neuronal N/C Ran ratio in control and two C9-ALS iPS lines show increased cytoplasmic Ran levels in untreated and scrambled antisense-oligonucleotide-treated C9-ALS iPSC neurons (n = 50 neurons per line. b, Salivary glands of larvae expressing G4C2 HRE and NLS–ΔNES–GFP were untreated (top) or treated with 5 µM antisense oligonucleotide (ASO, bottom) and co-stained for GFP (green), TO-PRO3 (blue) and antisense oligonucleotide (white). N, nuclear; W, whole cell. c, EMSA of RanGAP1 and repeat RNA in the presence of TMPyP4 (top panel) and relative change in fraction bound (bottom panel). d, e, Salivary glands of larvae expressing G4C2 HRE and NLS–ΔNES–GFP were treated with different concentrations of TMPyP4 (d) or KPT-276 (e) versus vehicle control and co-stained for GFP (green) and TO-PRO3 (blue). Scale bars, 20 µm. f, The effects of antisense oligonucleotide, KPT-276 and TMPyP4 on the external morphology of eyes expressing G4C2 repeats. *P < 0.05; **P < 0.01. All error bars indicate s.e.m.

Conclusions

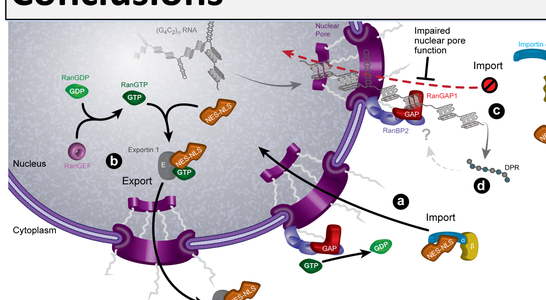

- **Expanded G_4C_2 RNA transcribed from the C9ORF72^{mut} allele aberrantly interacts with components of the nuclear pore and RanGAP1.**
- **RanGAP1:G_4C_2 RNA interaction impairs RanGAP1 activity resulting in a disrupted RanGTPase gradient and reduces nuclear import dynamics of proteins that contain a classical NLS (e.g. TDP-43) resulting in their cytoplasmic accumulation.**
- **Degrading the G_4C_2 RNA, blocking its ability to interact with proteins via small molecules, and nuclear export inhibitors rescues the observed nuclear import deficits.**